Photoresponsive microvalve for remote actuation and flow control in microfluidic devices

Amol D. Jadhav,[1] Bao Yan,[1] Rong-Cong Luo,[2] Li Wei,[1] Xu Zhen,[1] Chia-Hung Chen,[2] and Peng Shi[1,3,a)]
[1]*Department of Mechanical and Biomedical Engineering, City University of Hong Kong, Kowloon, Hong Kong 999077, China*
[2]*Department of Biomedical Engineering, National University of Singapore, Singapore 117575*
[3]*Shenzhen Research Institute, City University of Hong Kong, Shen Zhen 518057, China*

(Received 4 May 2015; accepted 18 June 2015; published online 30 June 2015)

Microvalves with different actuation methods offer great integrability and flexibility in operation of lab-on-chip devices. In this work, we demonstrate a hydrogel-based and optically controlled modular microvalve that can be easily integrated within a microfluidic device and actuated by an off-chip laser source. The microvalve is based on in-channel trapping of microgel particles, which are composed of poly(N-isopropylacrylamide) and polypyrrole nanoparticles. Upon irradiation by a near-infrared (NIR) laser, the microgel undergoes volumetric change and enables precisely localized fluid on/off switching. The response rate and the "open" duration of the microvalve can be simply controlled by adjusting the laser power and exposure time. We showed that the trapped microgel can be triggered to shrink sufficiently to open a channel within as low as ∼1–2 s; while the microgel swells to re-seal the channel within ∼6–8 s. This is so far one of the fastest optically controlled and hydrogel-based microvalves, thus permitting speedy fluidic switching applications. In this study, we successfully employed this technique to control fluidic interface between laminar flow streams within a Y-junction device. The optically triggered microvalve permits flexible and remote fluidic handling, and enables pulsatile *in situ* chemical treatment to cell culture in an automatic and programmed manner, which is exemplified by studies of chemotherapeutic drug induced cell apoptosis under different drug treatment strategies. We find that cisplatin induced apoptosis is significantly higher in cancer cells treated with a pulsed dose, as compared to continuous flow with a sustained dose. It is expected that our NIR-controlled valving strategy will provide a simple, versatile, and powerful alternative for liquid handling in microfluidic devices. [http://dx.doi.org/10.1063/1.4923257]

I. INTRODUCTION

Microfluidics enables transportation and control of fluid samples on miniaturized, or lab-on-chip, platforms that are employed for diverse applications in chemical and biological assays. In these systems, micromixers and micropumps are essential components for fluidic handling, and microvalves are the crucial control element for automation and large scale integration.[1] A variety of microvalves based on different actuation strategy, including magnetic, electric, pneumatic, piezoelectric, and thermal, have been reported for on-chip fluidic control.[2–9] While pneumatic microvalves allow multiplexed valving and can reach a density of 100/cm^2, the need for external controllers, solenoid valves, and the power requirements limits its utility to bench top operations, unless the portable version requires lower number of valves.[4,10,11] Most of the other

a)Author to whom correspondence should be addressed. Electronic mail: pengshi@cityu.edu.hk

types of microvalves demand time-consuming fabrication, require on-chip power, and complicated automation, making them difficult to be integrated with other platforms and limiting the portability as well as the operational flexibility. Several phase-change-based microvalves based on thermal, magnetic, or optical actuation have also been reported. Paraffin that has a solid to liquid volume expansion of 10%–30% can work as thermally actuated valves.[12–15] Sol-gel[16] valves based on pluronics or methyl cellulose have been demonstrated with switching time of ~1 s. Magnetic nanoparticles can form plugs in microchannels and are actuated by magnetic field.[17] Ionogel that incorporates ionic liquids with polymer gels also show good promise but has a very slow closing time.[18,19] Moreover, a variety of hydrogel based responsive microvalves have been fabricated by *in situ* photopolymerization. Many of these valving strategies depend on the composition of the hydrogels, which are incorporated with different additives, forming composites that can be tailored to enable reversible volumetric change in response to a variety of stimuli such as pH, electric, or magnetic field.[20]

Recently, integrated monolithic microvalves using photoresponsive hydrogels have gained great attention, because the actuation can simply be controlled by light irradiation from a remote source, thus eliminating any physical contact and offering significant improvement in versatility during microfluidic operation. Especially, photothermally responsive hydrogels for microvalving have been reported by several research groups, all of these studies use poly(N-isopropylacrylamide) (pNIPAM) as the polymeric material of choice. pNIPAM is a biomaterial with a lower critical solution temperature (LCST) about 37 °C. Below the LCST, pNIPAM hydrogel is hydrophilic, absorbs a high amount of water and exists in a transparent swollen state. When above the LCST, pNIPAM undergoes volumetric shrinkage and exists in a collapsed state.[21] This unique property has been exploited for applications in drug-delivery systems,[22] biomaterials,[23] and recently within microsystems technology as soft actuators and valves for controlling flow.[24] However, most of the studies focusing on photothermally responsive microvalves use polymeric plugs that are covalently attached to the wall of fluid channels through surface primer reagent, and acts as monolithic microvalve. A modular microvalve that can be introduced and replaced on demand as per experimental requirement has not been conceived and demonstrated yet. Furthermore, the ability to maximize volumetric change of the hydrogel with short irradiation time and lower power is vital for practical operation of an ideal microvalve.

Several materials such as iron oxide,[25–27] gold,[28,29] carbon nanotubes,[30,31] and graphene oxide[32] have been explored as photothermal transducing elements incorporated within the hydrogel matrix forming a nanocomposite. Organic nanomaterials such as spirobenzopyran[33] have been used as photothermal transducers within the pNIPAM matrix to enable relatively fast shrinkage but slow cooling and expansion, thus delayed closure of the microvalve. Gold nanorods (GNRs) pNIPAM gel capsule shell has been tested for their shrinkage swelling behavior, which showed anisotropic and slow swelling.[34] Also the low photostability of GNR and melting behavior upon multiple NIR-light exposure makes them unsuitable for faster operations.[35,36] Similarly, several studies that utilized graphene oxide as the transducing material have used NIR irradiation of several Watts over 1–2 min period to achieve valve opening.[32,37,38] Even though, Lee *et al*. recently developed a fast responding hydrogel incorporated with iron oxide nanoparticles that allowed rapid opening of the valve in as little as 9 s after exposure to blue light, the valve closing (volumetric relaxation) still took about 6–7 min.[27] It is important to note that such fast actuation was achieved after chemical manipulation of the matrix, not simply due to the presence of iron oxide nanoparticles. Although, all the above mentioned photoresponsive hydrogel nanocomposites show controlled and reproducible volume change, the long operation time and modest volume change limit their application as actuators or microvalves. Notably, none of these photoresponsive microvalves have demonstrated practical application of the flow control capability towards biological or chemical assays.

Polypyrrole (PPy), an organic conductive polymer is known for its high conductivity and outstanding stability.[39–41] PPy has good absorbance in the NIR range of wavelengths (800–1500 nm), it absorbs NIR radiation and converts the energy of the radiation into heat making them ideal photothermal agent for hydrogel microvalve actuation. PPy nanomaterials have

excellent biocompatibility and have been used in applications such as biosensors,[42] drug delivery,[43] neural tissue regeneration,[44–46] cancer phototherapy,[47,48] and optical coherence tomography (OCT) imaging. Especially, the thermal transduction capability and excellent chemical stability make PPy an ideal candidate for actuation applications, including valving in microfluidic devices.

In this paper, we report a modular microvalve that consists of pNIPAM matrix and PPy nanoparticles that act as embedded photothermal nanotransducers. Microgels with uniform diameters were prepared using droplet microfluidics as previously reported[49] and were characterized for their volumetric change upon irradiation with NIR 980 nm laser. Selected microgel was trapped within a microfluidic channel to act as a microvalve, and the valving performance was evaluated at different laser power and flow rates. Our results demonstrated one of the fastest optically actuated and hydrogel-based microvalves yet reported, with prompt opening response as little as ∼1–2 s, and closing response of around ∼6–8 s. To demonstrate the utility towards biological applications at physiologically relevant condition (pH = 7.4), we specifically applied our new technology to deliver pulsatile doses of chemotherapeutic drug to adenocarcinoma cells to study the calcium homeostasis and induced apoptosis. Further, in combination with the microLED technology that allows achieving placement of over 20 pixels/mm^2 and optical output power densities per pixel of 5 W/cm^2–20 W/cm^2, we think our photosensitive microvalve platform can be easily scaled for complicated multiplexed flow control schemes.[50,51] The fast response rate, ease-of-use and remote control capability of the system makes our modular microvalve attractive for applications in microfluidic circuits and cheap, portable point-of-care devices.

II. MATERIALS AND METHODS

A. Nanocomposite microgel fabrication

The microgels were fabricated using the procedure described previously.[49] Briefly, a Y-junction droplet microfluidic device was used for the microgel production. The aqueous solution was composed of a mixture containing monomer *N*-isopropylacrylamide (NIPAM), crosslinker *N*,*N*′-methylenebisacrylamide (BIS), and initiator ammonium persulfate (APS) (Sigma-Aldrich, Singapore) with a w/v ratio of 9.4%, 0.65% (or 0.85%), and 0.64%, respectively. This mixture was pumped through a channel of the Y-junction device at a flow rate 12 μl/min using a syringe pump. An aqueous solution of the PPy nanoparticles (250 μg/ml) was pumped through the other channel of the Y-junction at a rate of 2 μl/min. Prior to this, dynamic light scattering (DLS) was used to characterize the nanoparticles. The DLS results implied that the PPy nanoparticles had an average diameter of 85 nm and a polydispersity index (PDI) of 0.054, which indicates the proper dispersion of PPy nanoparticles in aqueous solution. The continuous phase consisted of fluorocarbon oil (HFE 7500, 3 M Novec Engineered Fluids) containing 2% (w/w) perfluorinated polyethers–polyethyleneglycol block copolymer (PFPE–PEG) surfactant and 7% (v/v) Tetramethylethylenediamine (TEMED) as the accelerator. TEMED is soluble in both the aqueous as well as oil phase, it diffuses from the oil phase into the aqueous droplets to initiate a redox reaction that polymerizes the NIPAM. Upon polymerization NIPAM solidifies, the composite microgels were separated from the oil phase by centrifugation at 4000 g for 5 min. After phase separation, the high density HFE7500 oil (1614 kg/m^3) and the microgels form the top layer in the centrifuge tube. The collected composite microgels were then washed with IPA and then several times with DI water to completely remove the residual IPA.

B. Scanning electron microscopy

Scanning electron microscopy images were obtained using an electron microscope (SEM XL30 FEG Philips). Briefly, the sample preparation involved critical point drying (EM CPD300, Leica, Germany) of the microgels, which can retain the nano/micro structure of samples during the dehydration process by avoiding surface tension effects. After sputter coating

with a thin film of gold, SEM images were captured and analyzed to determine the exact size of the synthesized microgels and their the pore sizes.

C. Microfluidic device fabrication

The microfluidic chip was made by assembling a PDMS molded device onto a glass cover slip. The PDMS was replica molded from a silicon mold with microscale patterns, which consisted of two SU-8 (Microchem) layers on a silicon wafer. The first layer contained negative features for the trapping area (60–70 μm height). The second layer of SU-8 contained features for the microchannel (30 μm). The two layers of photoresist were patterned sequentially using standard photo-lithography (Karl Suss, MA6). To create the device, the pre-polymer was then poured onto the silane-treated (trichloro-perfluorooctyl silane, Sigma) wafer with the SU-8 patterns, and degassed. The assembly was placed in a temperature-controlled oven and allowed to cure for at least 12 h at 80 °C, on curing the device was gently peeled off from the master mold. The clean microfluidic device and sterile glass coverslips were plasma treated for 5 min prior to the assembly of the device. The adhesion between PDMS and the coverslip surface was strong enough to prevent solution leaking during operation.

D. Microvalve assembly

Uniform sized microgels were washed several times with distilled water followed by loading a few into the inlet chamber using a standard 10 μl pipette. This was followed by fluid pumping to push the microgel into the trapping area. The gel is squeezed as it passes through the flow channels and expands on reaching the trapping area, occupying the space, and sealing the channel (see supplementary Video S1 in Ref. 63). To avoid trapping of the remaining micorogels into the channel, a reverse fluid flush was performed from the side of the inlet chamber removing all the extra material.

E. Laser stimulation and image acquisition

The laser diode driver was used to stimulate the microvalve. The laser power was measured using Photodiode Power Sensor (S146C, Thorlabs). All images were obtained using an inverted microscope (IX81, Olympus) equipped with a sCMOS camera (Andor, Neo).

F. Characterization of the photothermally responsive microgel

The microgel particles were placed in a culture dish with glass bottom in water (with 1% tween-20), pH 7.4. The laser was aligned with the objective to enable stimulation of the microgel particle with simultaneous microscopic visualization. Different laser power settings 0.5 W, 1 W, 1.5 W, 2 W, and 2.5 W (equivalent to power densities of 100 mW/cm^2, 200 mW/cm^2, 300 mW/cm^2, 400 mW/cm^2, and 500 mW/cm^2 at exposure plane, respectively) and exposure timings (10 s, 30 s, 45 s, and 60 s) were tested. For evaluating the change in size upon stimulation, time series of microscopic images were recorded at a frame rate of 20 Hz and analyzed later. At least 4–5 trials were performed to confirm the reproducibility.

G. Functional evaluation of the microvalve in a Y-shape device

The Y-shape microfluidic device fabricated by casting in PDMS was used for characterizing the microvalve capability. Briefly a single microgel was held within the trapping area followed by pumping of color dye through the free flow channel and water in the microvalve controlled channel. Laser stimulation was applied (optic fiber with a collimating lens placed close to the valve area) to actuate the microvalve accompanied by simultaneous imaging of the flow streams in the main channel using an inverted microscope (IX81, Olympus).

H. Cell culture and drug treatment

A549 cells cultured in 4 well plates and well as in the microfluidic chip. The central channel of the microfluidic chamber was seeded at a density of $8–10 \times 10^6$ cells/ml. After initial adhesion of the cells (2 h after seeding), the medium was replaced by DMEM medium supplemented with L-glutamine and penicillin/streptomycin. Half of the medium was replaced with fresh medium every 8–10 h. The cells were allowed to culture for 3–4 days prior to the cytotoxicity assay. For control experiments, we exposed the cell with different concentration of Cisplatin (0, 24, 50 μM) for a period of 2 h, followed by live-dead cell staining after 6–24 h. For pulsed treatment, a continuous perfusion of PBS was maintained in the central channel where the cells are. The microvalve was stimulated and kept open for 120 s followed by a 180 s OFF period, thus allowing pulsatile treatment in one half of cells for 90–120 min. The cells were washed with PBS after the treatment and placed within growth media for at least 6–24 h before further analysis.

I. Live/dead imaging for cell viability

Cell viability kit was purchased from Life technologies. The cells were incubated for 30 min in the working solution containing 2 μM Calcein-AM and 4 μM EthD-1, followed by washing and fluorescence imaging in a temperature controlled chamber.

III. RESULTS AND DISCUSSION

In order to exploit the photoresponsive capability of our nanocomposite microgel and the modularity it offers as a microvalve, we implemented a simple microfluidic switching scheme. The operation principle is illustrated in Fig. 1, a nanocomposite microgel was held in the trapping area within a channel, blocking the fluidic flow before the laser exposure. Once the NIR laser was turned ON, the microgel underwent volumetric shrinkage and allowed the flow of liquid. The microvalve

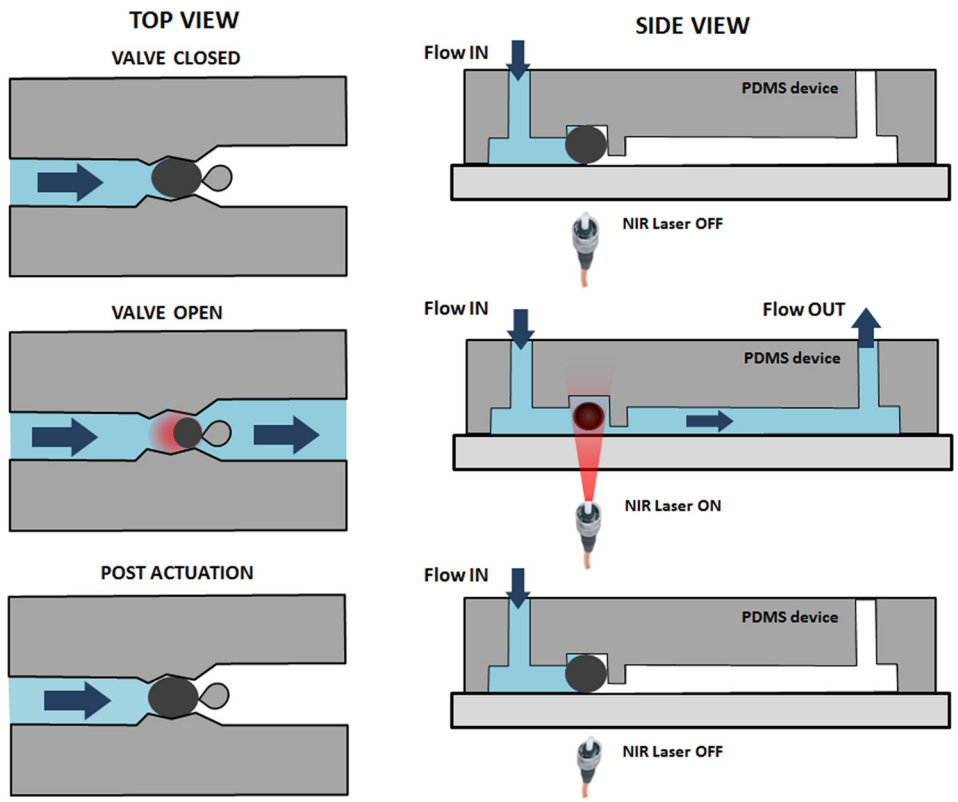

FIG. 1. Schematic showing the assembly and operation of our photoresponsive hydrogel microvalve. Irradiation with a NIR 980 nm laser actuates the trapped microgel and allows flow switching in microfluidic devices.

relaxed to its original size once the laser was switched off and resealed the channel. The whole control operation was performed remotely with minimal interference, and the photoresponsive hydrogel based microvalve has a fast response rate and can be actuated in a repeatable manner.

A. Characterization of the photoresponsive microgel

The structure material of the nanocomposite is pNIPAM, a thermally responsive polymer with a lower critical solution temperature (LCST) about 37 °C. When heated above its LCST, pNIPAM undergoes volumetric shrinkage as it undergoes coil-to-globule transition and changes from a hydrophilic to a hydrophobic state, expelling water molecules.[21,52] This transition is reversible and swelling occurs once the temperature is decreased below LCST. PPy nanoparticles incorporated into the structural hydrogel work as photothermal nanotransducers (see supplementary Fig. S1 in Ref. 63). The PPy nanoparticles were synthesized as described previously,[49] using a microemulsion method in the aqueous phase with $FeCl_3$ as the oxidizing agent and poly(vinyl alcohol) (PVA) as the stabilizer. PPy nanoparticles have very good stability even under varying pH conditions, and they are stable for several weeks in an acidic or weakly basic solution.[53] Upon NIR irradiation, the embedded PPy nanoparticles cause temperature rise inside the microgel matrix and shrinkage of the microgel above LCST.[54,55] The photoresponsive efficiency of the microgel depends on three parameters: PPy nanoparticle concentration, crosslinking degree of pNIPAM, and the laser irradiation power, which can be, respectively, optimized. Higher concentration of PPy nanoparticles leads to higher temperature rise upon irradiation and thus faster response, similarly increasing the power can also lead to faster actuation for a certain concentration of PPy nanoparticles within the nanocomposite. The microgel used for this work was approximately 100 μm in diameter, as shown in Fig. 2(a). The photoresponsive properties of the microgel that influence the valve opening-closing response rate can be tuned by simply changing the PPy concentration within the hydrogel nanocomposite, or the crosslinking degree of pNIPAM.

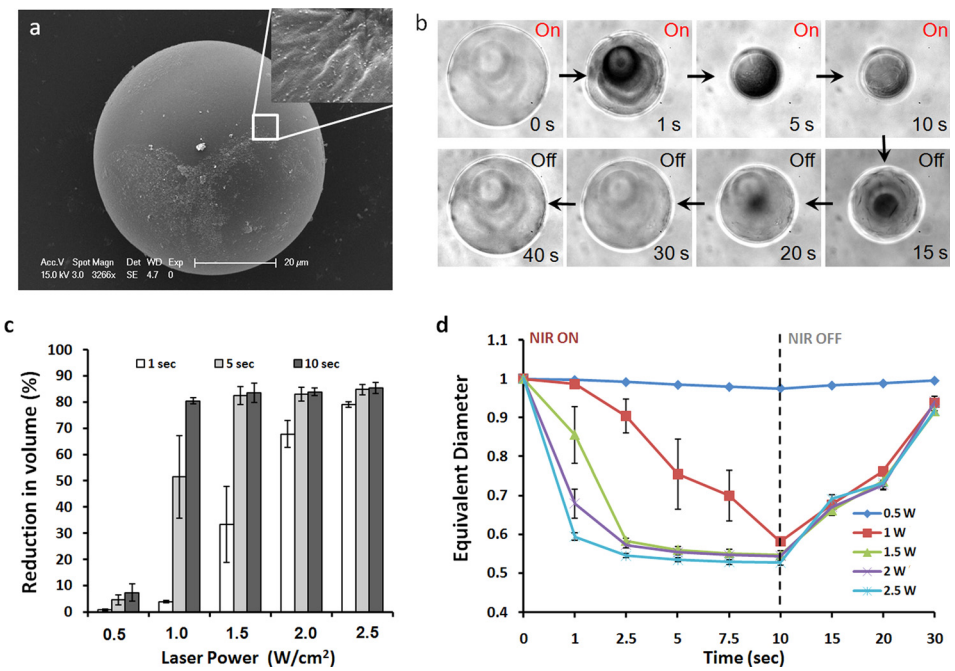

FIG. 2. Characterization of modular photoresponsive hydrogel based microvalve unit. (a) SEM image of a single composite microgel. (b) Swelling, de-swelling of a single microgel during stimulation with NIR (2 W at laser source, equivalent power density 400 mW/cm^2 at exposure plane). (c) Percentage change in volume of the microgel at different irradiation time. (d) Graph showing the equivalent diameter of the pNIPAM-PPy microgel during shrinking and swelling conducted at different power.

As a proof of principle to demonstrate the feasibility of microgel based actuation, we decided to employ particles with a cross-linking degree of 8.5. A 980 nm NIR laser was used to activate the embedded PPy nanoparticles and to elevate the temperature within the nanocomposite, which in turn induced volumetric change of the microgel. The microgels exhibit fast volumetric shrinkage, within first 2–3 s of irradiation above power exceeding 1 W (power density of 200 mW/cm^2 at exposure plane). As shown in Fig. 2(b), the microgel shows fast response and recovery as soon as the laser is switched off. At irradiation power of 1.5 W (300 mW/cm^2), the microgels exhibited significant decrease in size: 10 s of irradiation could reduce the diameter by more than 40%, which is equivalent to over 80% reduction in volume. At higher laser power (2.5 W, equivalent power density of 500 mW/cm^2), the overall volumetric change was even faster, 1–2 s irradiation was enough to collapse the microgel (Figs. 2(c) and 2(d)). In order to achieve faster response time suitable for quick flow switching, we chose optimum laser intensity in the range of 1.5–2.5 W (300–500 mW/cm^2), this enabled extended period of actuation without damaging the microvalve. The irradiation power is not dramatically higher compared to previously reported photo-responsive actuators. For example, Zhu *et al* utilized 808 nm laser of 2 W for stimulator the pNIPAM-graphene oxide nanocomposite based microvalve;[32] Lee *et al.* employed a power of 380 mW/cm^2 to achieve flow switching within ∼5 s.[27] In addition to power control, there are two factors can also contribute to the fast response of our pNIPAM-PPy microvalves: 1) the good absorption of NIR energy by PPy nanoparticles; 2) the midscale size the composite microgels and uniform distribution of nanoparticles within the microgel, which resulted from the droplet-based microemulsion method (see supplementary Fig. S2 in Ref. 63).

B. Remote control of fluid flow using the photoresponsive microvalve

A simple Y-junction microfluidic device was used to evaluate the valving capability of the modular microgel. As shown in Fig. 3(a), a single microgel was confined within the trapping

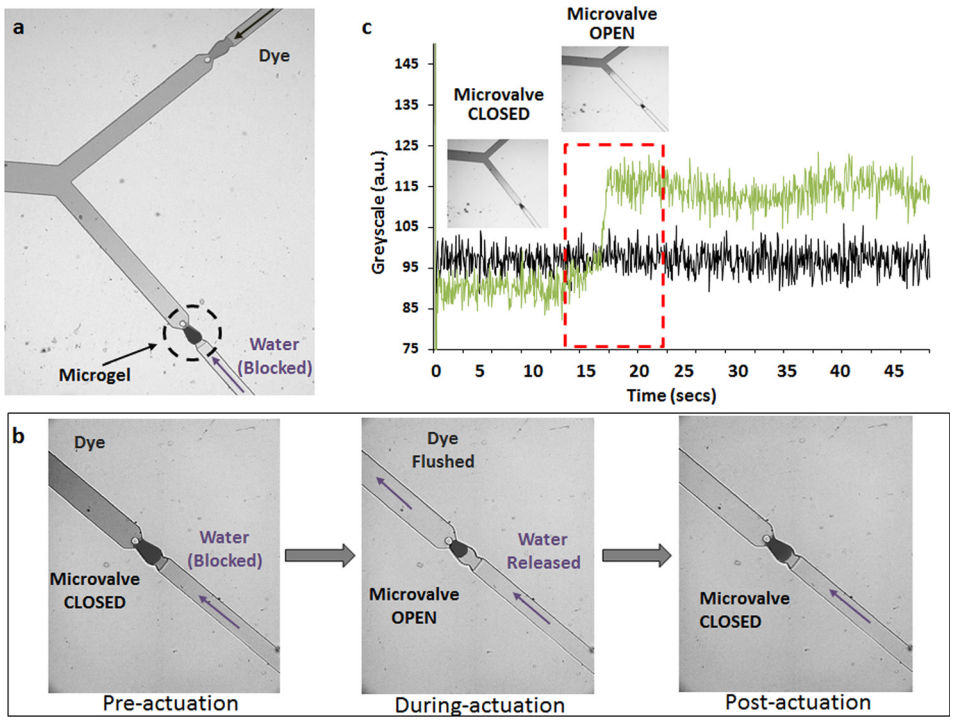

FIG. 3. Remote stimulation and control of flow on microfluidic chip. (a) A trapped microgel shows uniform sealing and prevents flow. (b) Microvalve status during operation, stimulation conducted at absolute power 2.5 W (equivalent power density of 500 mW/cm^2) for 10 s. (c) Graph showing change in grey value pixels within the water channel (top inlet of the Y-channel device) during microvalve operation.

area in one of the two inlets of the Y-channel device, and the fluid behavior within the main channel was monitored through microscopic imaging. To test the capability of the microvalve to seal flow in either direction of the channel, we pumped red dye through the open inlet and plain water in microgel-loaded inlet channel at various flow rates ranging from 1 ml/h to 15 ml/h. The microvalve was able to completely block the flow from the channel. Higher flow rate (>10 ml/h) would dramatically deform the microgel against the holding post, but the microgel still remained intact and could still be repeatedly used for valving with optical actuation. Fig. 3(b) shows a microvalve in action, the dye in the lower channel was flushed on opening of the valve. At the irradiation power of 2.5 W (equivalent power density of 500 W/cm^2 at exposure plane), a few seconds NIR exposure was sufficient to open the water channel and to flush out the dye that originally occupied the channel (Figs. 3(b) and 3(c)). The flow discharge from the microgel-loaded inlet channel was very fast, and it took as little as ~1–2 s for the water to enter the main channel to establish a stable interface with two parallel laminar streams within the main channel (Fig. 4, also see supplementary Video S2 in Ref. 63). The other unique capability of this microgel is their ability to quickly reseal and completely stop the flow; we found that this could be achieved in about 6–8 s after the laser was turned off. When the microvalve was optically controlled to maintain "OPEN" status, the laminar flow in the main channel showed similar behavior as the flow in another device with both inlet channels unrestricted (Fig. 4(a)). Despite the fact that hydrogels such as pNIPAM absorb water and this can be an issue for valving applications there have several examples showing the application of such composite gels as microvalves,[27,38,51] the ability to control the pore size and degree of crosslinking can help reduce the potential diffusion from the closed stream.

Apart from the capability to quickly discharge the flow, it is also important that the microvalve can promptly switch OFF the flow by re-sealing the channel. Even though we did not apply any approaches to control the swelling rate of the microgel after NIR-stimulated shrinking, we specifically used shorter period of laser irradiation that allowed just enough shrinkage of the microvalve to permit flow. Such small volumetric change, along with the microscale size of the gel particles, helped to achieve fast recovery and subsequent sealing of fluid channels, enhancing the operation speed of the microvalve.

C. Pulsed drug treatment using the photoresponsive microvalve

Since the focus of this work was to develop photothermally sensitive pNIPAM based fluid switching element for biological assays, the operational environments were mostly physiologically relevant conditions (e.g., pH and temperature). To demonstrate the practical application of our platform towards fluid switching, we then employed the photoresponsive microvalve to perform drug treatment on cancer cells cultured within a Y-shape device. Microfluidic devices enable studying the cellular responses to chemical or biomolecular stimulation in a controlled manner. The parallel flows that are developed in the main cell culture channel within the Y-shape device enable observing the dynamic effect by fluidically patterning the chosen area of the culture, which is not possible using traditional plate based cell culture. Therefore, the micro-environmental effects on adjacent cells (with similar growth conditions) can be readily studied. The presence of microvalve not only allowed precise sealing and isolation of the drug channel but also demonstrated the capability to control it using off-chip stimulation. Such autonomous microvalving strategy would be important for scaling up operations using lab-on-chip devices, which might otherwise require programmable instrumentation and multiple syringe pumps. In this study, different dosing strategies, including programed pulsatile treatment and continuous perfusion, were tested to investigate cisplatin-induced apoptosis in A549 cells. Cisplatin is a chemotherapeutic agent that is generally recognized as a DNA-damaging drug but it can also induce apoptosis through endoplasmic reticulum (ER), a non-nuclear target.[56] As shown in Figs. 5(a) and 5(b), 2 h Cisplatin treatment induced significant cell death in area covered by drug-containing stream in the laminar flow system. Interestingly, we found that pulsatile treatment of Cisplatin was much more effective in killing cancer cells than continuous flow with a sustained dose (Fig. 5(c)). It should be noted that the microgel area that was stimulated

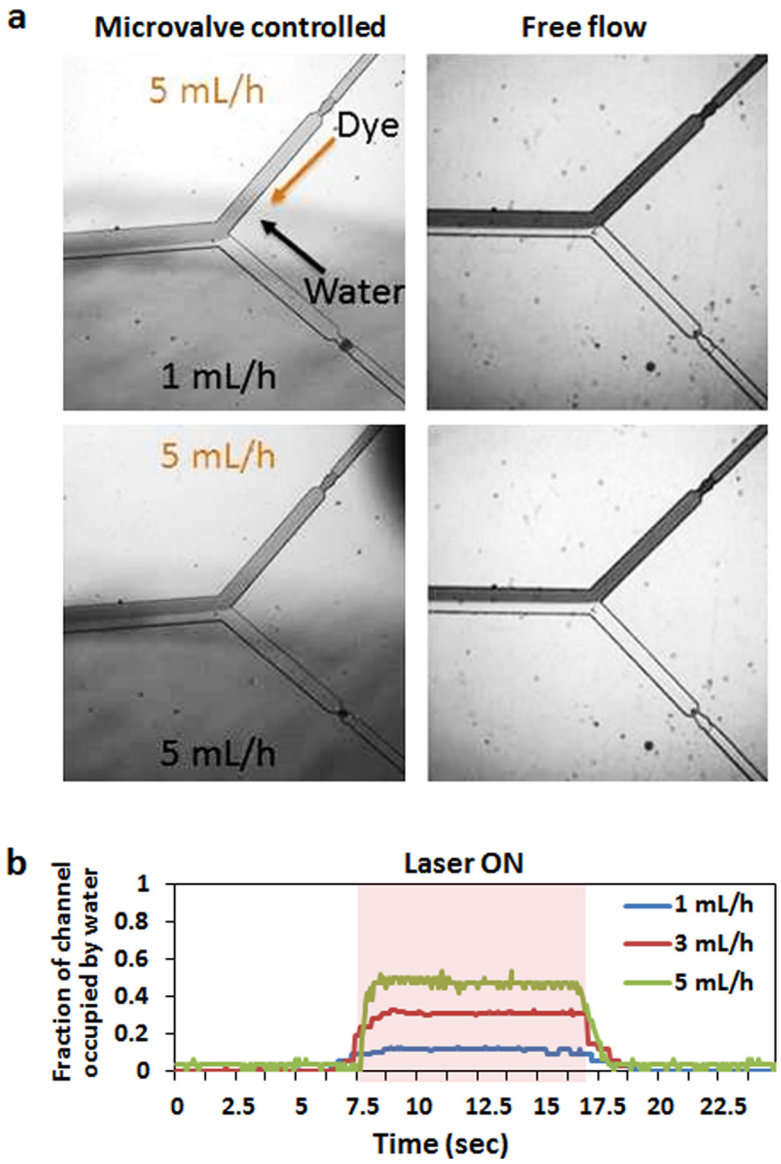

FIG. 4. Fluid flow remotely controlled by NIR actuated microvalve. (a) Comparison of fluid boundaries generated within a Y-channel microfluidic device, microvalve open, and free flow (no valve) conditions. (b) Graph showing the fraction of main channel occupied by water (change of interface between laminar flows) during laser microvalve operation. NIR irradiation period is indicated by red-shaded area. The flow rate in the dye channel (top inlet of the Y-channel device) was kept constant 5 ml h^{-1}, while the water channel was varied as shown.

was several hundred microns away from the cell culture area, thus avoiding any thermal effects on to cells, besides the microgels did not show any degradation that might lead to PPy mediated toxicity. Cisplatin-induced genotoxic stress activates multiple signal transduction pathways, which can contribute to apoptosis or chemoresistance. Several studies have shown that low level or sustained long term exposure make the cancer cells resistant to cisplatin due to defect in apoptotic pathway, whereas medium dose and short treatment period achieved maximal apoptosis in cancer cells.[57–60]

As cisplatin induces apoptosis and increases calcium in different cancer cell lines,[61,62] we then implemented our flow control scheme to provide pulsed cisplatin treatment and to verify the changes in calcium homeostasis. Our results indicated that the cyclical extracellular cisplatin treatment can cause elevation of intracellular calcium level after 15–30 min (see supplementary

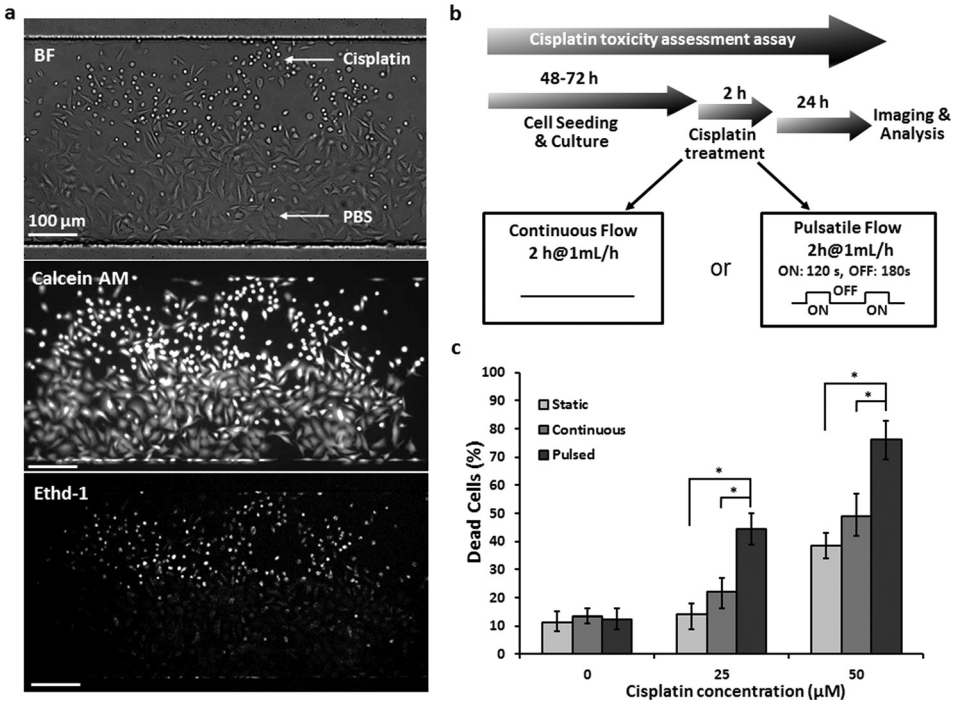

FIG. 5. On-chip spatially and temporally selective drug treatment enabled by NIR-actuated microvalves. (a) Live/dead staining of A549 cells after on-chip cisplatin treatment. Scale bar, 100 μm. (b) Schematic showing the experimental protocol and drug treatment patterns: continuous flow for 2 h, or pulsatile flow for 2 h (2 min ON, 3 min OFF). (c) Quantification of cell death 24 h post drug exposure verified by live-dead assays. Three independent experiments were conducted, error bars indicate s.e.m., *$P < 0.001$ by student-t test.

Fig. S3 and Video S3 in Ref. 63), which is possibly associated with elevated intracellular stress and increased cell death with pulsed treatment.

IV. CONCLUSION

We developed a modular microvalve platform based on photoresponsive hydrogel that can be easily integrated with microfluidic device and controlled by external optical triggers. The microvalve was based on pNIPAM-PPy microgels, which were first characterized for their shrinking/swelling response at different laser irradiation settings. The valving function was achieved through the volumetric change of microgels trapped in microfluidic devices, which typically showed over 80% reduction in volume within 10 s of irradiation. However, a small volume change induced by a much shorter NIR exposure was sufficient to switch the flow status. When implemented within a Y-junction microfluidic device the opening response and fluid discharge could be achieved within as little as 1–2 s, making these the fastest optically controlled microvalves yet reported. Additionally, the closure can be achieved within ~6–8 s, also several times faster than any previously reported results.[27,38] We anticipate that combining such modular photothermal microvalve system with programmable microLEDs can enable scaling up the operation to multiple microvalves simultaneously or sequentially to achieve flow control within lab-on-chip platforms.

Further for a proof-of-concept demonstration, we tested the capability of the assembled microvalve to maintain laminar flow and pulsed liquid stream within microfluidic devices, which was subsequently used to treat cells with a chemotherapeutic drug using different flow patterns. The results show that lung adenocarcinoma cells can achieve apoptosis faster when exposed to cisplatin in a pulsatile manner and at higher dosage. The mortality rate of the treated cells was more than 80% in case of pulsed flow, and such rate was much lower with continuous flow treatment under static condition. Notably, the microgel-based valving element

is triggered ON/OFF via remotely coupled NIR irradiation, which not only enables off-chip control but can also pave way for developing complicated microfluidic circuits for practical application in life sciences and portable point-of-care diagnostics.

ACKNOWLEDGMENTS

This work was supported by the National Science Foundation of China (81201164), University Grants Council of Hong Kong (ECS125012, GRF11211314), Innovation and Technology Commission of Hong Kong (ITF3 ITS/376/13) and grants from the City University of Hong Kong (9667120).

[1]K. W. Oh and C. H. Ahn, J. Micromech. Microeng. **16**(5), R13 (2006).
[2]S. Shoji and M. Esashi, J. Micromech. Microeng. **4**(4), 157 (1994).
[3]R. B. Schasfoort, S. Schlautmann, J. Hendrikse, and A. van den Berg, Science **286**(5441), 942–945 (1999).
[4]M. A. Unger, H.-P. Chou, T. Thorsen, A. Scherer, and S. R. Quake, Science **288**(5463), 113–116 (2000).
[5]S. Böhm, G. Burger, M. Korthorst, and F. Roseboom, Sens. Actuators, A **80**(1), 77–83 (2000).
[6]E. T. Carlen and C. H. Mastrangelo, J. Microelectromech. Syst. **11**(5), 408–420 (2002).
[7]S. Z. Hua, F. Sachs, D. X. Yang, and H. D. Chopra, Anal. Chem. **74**(24), 6392–6396 (2002).
[8]W. H. Grover, R. H. Ivester, E. C. Jensen, and R. A. Mathies, Lab Chip **6**(5), 623–631 (2006).
[9]C.-Y. Chen, C.-H. Chen, T.-Y. Tu, C.-M. Lin, and A. M. Wo, Lab Chip **11**(4), 733–737 (2011).
[10]K. A. Addae-Mensah, Y. K. Cheung, V. Fekete, M. S. Rendely, and S. K. Sia, Lab Chip **10**(12), 1618–1622 (2010).
[11]J. D. Tice, T. A. Bassett, A. V. Desai, C. A. Apblett, and P. J. Kenis, Sens. Actuators, A **196**, 22–29 (2013).
[12]P. Selvaganapathy, E. Carlen, and C. Mastrangelo, Sens. Actuators, A **104**(3), 275–282 (2003).
[13]L. Klintberg, M. Karlsson, L. Stenmark, and G. Thornell, Sens. Actuators, A **105**(3), 237–246 (2003).
[14]R. Pal, M. Yang, B. N. Johnson, D. T. Burke, and M. A. Burns, Anal. Chem. **76**(13), 3740–3748 (2004).
[15]J.-C. Yoo, Y. Choi, C. Kang, and Y.-S. Kim, Sens. Actuators, A **139**(1), 216–220 (2007).
[16]Y. Liu, C. B. Rauch, R. L. Stevens, R. Lenigk, J. Yang, D. B. Rhine, and P. Grodzinski, Anal. Chem. **74**(13), 3063–3070 (2002).
[17]K. W. Oh, K. Namkoong, and P. Chinsung, in *Proceedings of microTAS 2005* (2005).
[18]F. Benito-Lopez, R. Byrne, A. M. Răduţă, N. E. Vrana, G. McGuinness, and D. Diamond, Lab Chip **10**(2), 195–201 (2010).
[19]F. Benito-Lopez, M. Antoñana-Díez, V. F. Curto, D. Diamond, and V. Castro-López, Lab Chip **14**(18), 3530–3538 (2014).
[20]B. D. Kieviet, P. M. Schön, and G. J. Vancso, Lab Chip **14**(21), 4159–4170 (2014).
[21]D. Ito and K. Kubota, Macromolecules **30**(25), 7828–7834 (1997).
[22]M. Bikram and J. L. West, Expert Opin. Drug Delivery **5**, 1077–1091 (2008).
[23]S. B. Campbell and T. Hoare, Curr. Opin. Chem. Eng. **4**, 1–10 (2014).
[24]L. Dong and H. Jiang, Soft Matter **3**(10), 1223–1230 (2007).
[25]J. Yoon, P. Bian, J. Kim, T. J. McCarthy, and R. C. Hayward, Angew. Chem. **124**(29), 7258–7261 (2012).
[26]C. H. Zhu, Y. Lu, J. F. Chen, and S. H. Yu, Small **10**(14), 2796–2800 (2014).
[27]E. Lee, H. Lee, S. I. Yoo, and J. Yoon, ACS Appl. Mater. Interfaces **6**(19), 16949–16955 (2014).
[28]S. R. Sershen, G. A. Mensing, M. Ng, N. J. Halas, D. J. Beebe, and J. L. West, Adv. Mater. **17**(11), 1366–1368 (2005).
[29]A. Shiotani, T. Mori, T. Niidome, Y. Niidome, and Y. Katayama, Langmuir **23**(7), 4012–4018 (2007).
[30]T. Fujigaya, T. Morimoto, Y. Niidome, and N. Nakashima, Adv. Mater. **20**(19), 3610–3614 (2008).
[31]X. Zhang, C. L. Pint, M. H. Lee, B. E. Schubert, A. Jamshidi, K. Takei, H. Ko, A. Gillies, R. Bardhan, and J. J. Urban, Nano Lett. **11**(8), 3239–3244 (2011).
[32]C. H. Zhu, Y. Lu, J. Peng, J. F. Chen, and S. H. Yu, Adv. Funct. Mater. **22**(19), 4017–4022 (2012).
[33]S. Sugiura, K. Sumaru, K. Ohi, K. Hiroki, T. Takagi, and T. Kanamori, Sens. Actuators, A **140**(2), 176–184 (2007).
[34]H. Lee, Chem. Commun. **49**(18), 1865–1867 (2013).
[35]S. Link, C. Burda, B. Nikoobakht, and M. El–Sayed, J. Phys. Chem. B **104**(26), 6152–6163 (2000).
[36]S. Link, Z. L. Wang, and M. A. El-Sayed, J. Phys. Chem. B **104**(33), 7867–7870 (2000).
[37]C.-W. Lo, D. Zhu, and H. Jiang, Soft Matter **7**(12), 5604–5609 (2011).
[38]D. Kim, H. S. Lee, and J. Yoon, RSC Advances **5**, 13867–13870 (2014).
[39]G. Heywang and F. Jonas, Adv. Mater. **4**(2), 116–118 (1992).
[40]K. Cheah, M. Forsyth, and V.-T. Truong, Synth. Met. **94**(2), 215–219 (1998).
[41]J. Y. Hong, H. Yoon, and J. Jang, Small **6**(5), 679–686 (2010).
[42]M. Gerard, A. Chaubey, and B. Malhotra, Biosens. Bioelectron. **17**(5), 345–359 (2002).
[43]S. Geetha, C. R. Rao, M. Vijayan, and D. Trivedi, Anal. Chim. Acta **568**(1), 119–125 (2006).
[44]R. T. Richardson, B. Thompson, S. Moulton, C. Newbold, M. G. Lum, A. Cameron, G. Wallace, R. Kapsa, G. Clark, and S. O'Leary, Biomaterials **28**(3), 513–523 (2007).
[45]S. M. Willerth and S. E. Sakiyama-Elbert, Adv. Drug Delivery Rev. **59**(4), 325–338 (2007).
[46]R. T. Richardson, A. K. Wise, B. C. Thompson, B. O. Flynn, P. J. Atkinson, N. J. Fretwell, J. B. Fallon, G. G. Wallace, R. K. Shepherd, and G. M. Clark, Biomaterials **30**(13), 2614–2624 (2009).
[47]Z. Zha, X. Yue, Q. Ren, and Z. Dai, Adv. Mater. **25**(5), 777–782 (2013).
[48]K. Yang, H. Xu, L. Cheng, C. Sun, J. Wang, and Z. Liu, Adv. Mater. **24**(41), 5586–5592 (2012).
[49]R.-C. Luo, S. Ranjan, Y. Zhang, and C.-H. Chen, Chem. Commun. **49**(72), 7887–7889 (2013).
[50]Z. Gong, E. Gu, S. Jin, D. Massoubre, B. Guilhabert, H. Zhang, M. Dawson, V. Poher, G. Kennedy, and P. French, J. Phys. D: Appl. Phys. **41**(9), 094002 (2008).

[51]A. Zarowna-Dabrowska, S. L. Neale, D. Massoubre, J. McKendry, B. R. Rae, R. K. Henderson, M. J. Rose, H. Yin, J. M. Cooper, and E. Gu, Opt. Express **19**(3), 2720–2728 (2011).
[52]C. Wu and S. Zhou, Macromolecules **28**(24), 8381–8387 (1995).
[53]D. Samanta, J. L. Meiser, and R. N. Zare, Nanoscale **7**(21), 9497–9504 (2015).
[54]E. Lopez-Cabarcos, D. Mecerreyes, B. Sierra-Martin, M. Romero-Cano, P. Strunz, and A. Fernandez-Barbero, Phys. Chem. Chem. Phys. **6**(7), 1396–1400 (2004).
[55]F. Li, M. A. Winnik, A. Matvienko, and A. Mandelis, J. Mater. Chem. **17**(40), 4309–4315 (2007).
[56]A. Mandic, J. Hansson, S. Linder, and M. C. Shoshan, J. Biol. Chem. **278**(11), 9100–9106 (2003).
[57]V. B. Cetintas, A. S. Kucukaslan, B. Kosova, A. Tetik, N. Selvi, G. Cok, C. Gunduz, and Z. Eroglu, Cell Biol. Int. **36**(3), 261–265 (2012).
[58]J.-H. Ren, W.-S. He, L. Nong, Q.-Y. Zhu, K. Hu, R.-G. Zhang, L.-L. Huang, F. Zhu, and G. Wu, Cancer Biother. Radiopharm. **25**(1), 75–80 (2010).
[59]K. Schrödl, H. Oelmez, M. Edelmann, R. M. Huber, and A. Bergner, Cellular Oncol. **31**(4), 301–315 (2009).
[60]Y. Wang, X. Tang, X. Feng, C. Liu, P. Chen, D. Chen, and B.–F. Liu, Anal. Bioanal. Chem. **407**, 1139–1148 (2015).
[61]F. Splettstoesser, A. M. Florea, and D. Büsselberg, Br. J. Pharmacol. **151**(8), 1176–1186 (2007).
[62]X. Liang and Y. Huang, Biosci. Rep. **20**(3), 129–138 (2000).
[63]See supplementary material at http://dx.doi.org/10.1063/1.4923257 for photoresponsive microvalve for remote actuation and flow control in microfluidic devices.